HHS Public Access

Author manuscript

Toxicol Appl Pharmacol. Author manuscript; available in PMC 2023 June 09.

Published in final edited form as:

Toxicol Appl Pharmacol. 2023 April 01; 464: 116436. doi:10.1016/j.taap.2023.116436.

Examination of the exposome in an animal model: The impact of high fat diet and rat strain on local and systemic immune markers following occupational welding fume exposure

K.A. Roach[a,*,1], **V. Kodali**[b], **M. Shoeb**[b], **T. Meighan**[b], **M. Kashon**[c], **S. Stone**[d], **W. McKinney**[d], **A. Erdely**[b], **P.C. Zeidler-Erdely**[b], **J.R. Roberts**[a], **J.M. Antonini**[b]

[a]Allergy and Clinical Immunology Branch (ACIB), National Institute of Occupational Safety and Health (NIOSH), Morgantown, WV USA

[b]Pathology and Physiology Research Branch (PPRB), National Institute of Occupational Safety ana Health (NIOSH), Morgantown, WV, USA

[c]Bioanalytics Branch (BB), National Institute of Occupational Safety and Health (NIOSH), Morgantown, WV, USA

[d]Physical Effects Research Branch (PERB), National Institute of Occupational Safety and Health (NIOSH), Morgantown, WV, USA

Abstract

The goal of this study was to investigate the impact of multiple exposomal factors (genetics, lifestyle factors, environmental/occupational exposures) on pulmonary inflammation and corresponding alterations in local/systemic immune parameters. Accordingly, male Sprague Dawley (SD) and Brown Norway (BN) rats were maintained on either regular (Reg) or high fat (HF) diets for 24wk. Welding fume (WF) exposure (inhalation) occurred between 7 and 12wk. Rats were euthanized at 7 12, and 24wk to evaluate local and systemic immune markers corresponding to the baseline, exposure, and recovery phases of the study, respectively. At 7wk, HF-fed animals exhibited several immune alterations (blood leukocyte/neutrophil number, lymph node B cell proportionality)—effects which were more pronounced in SD rats. Indices of lung injury/inflammation were elevated in all WF-exposed animals at 12wk; however, diet appeared to preferentially impact SD rats at this time point, as several inflammatory markers (lymph node cellularity, lung neutrophils) were further elevated in HF over Reg animals. Overall, SD rats exhibited the greatest capacity for recovery by 24wk. In BN rats, resolution of immune alterations was further compromised by HF diet, as many exposure-induced alterations in local/systemic immune markers were still evident in HF/WF animals at 24wk. Collectively, HF diet appeared to have a greater impact on global immune status and exposure-induced lung injury in SD rats,

*Corresponding author at: National Institute of Occupational Safety and Health (NIOSH), 1095 Willowdale Drive, MS4020, Morgantown, WV 26505, USA. WVQ1@cdc.gov (K.A. Roach).

[1]Mailing Address: 1000 Frederick Lane, Morgantown, WV 26508, USA.

Declaration of Competing Interest

The authors declare no potential conflicts of interest with respect to the research, authorship, and/or publication of this article.

Appendix A. Supplementary data

Supplementary data to this article can be found online at https://doi.org/10.1016/j.taap.2023.116436.

but a more pronounced effect on inflammation resolution in BN rats. These results illustrate the combined impact of genetic, lifestyle, and environmental factors in modulating immunological responsivity and emphasize the importance of the exposome in shaping biological responses.

Keywords

Exposome; High fat diet; In vivo model; Immunotoxicity; Welding fume; Occupational health

1. Introduction

The term “exposome” was first used in 2005 to describe the totality of all external, internal, and non-specific exposures an organism is subjected to within its lifetime, and correspondingly, how these exposures influence various health outcomes (Wild, 2005). The impact of the exposome in human health and disease has become an area of active scientific investigation in recent years, as it becomes increasingly recognized that most chronic health conditions and disease states emerge as a result of combinations of various risk factors, internal and external stressors, and multidimensional interactions between such influences (Martin-Sanchez et al., 2020). Moreover, since many chronic health conditions remain poorly-understood from an etiological stand-point, it has been suggested that advancing our understanding of the exposome may represent a potential avenue by which more efficacious preventative strategies, diagnostic tools, and treatment options can be developed and implemented to improve health outcomes in various populations (Carlsten, 2018).

Major components of the exposome include specific environmental exposures (e.g., pollution, pathogens, drugs), general external influences (e.g., socioeconomic status, climate), lifestyle and behavioral factors (e.g., unhealthy diet, smoking, lack of exercise), genetic influences, and internal exposures (e.g., microbiome alterations, chronic inflammation) (Fang et al., 2021). These ubiquitous influences render the exposome inherently dynamic and tremendously variable throughout the course of a lifetime, and thus, exceedingly difficult to study in human subjects (Robinson and Vrijheid, 2015). Because of these limitations, animal models have become an invaluable tool frequently employed by toxicologists to study various aspects of the exposome in a controlled setting (Antonini et al., 2019a). As a result, the exposome has been examined in the context of many different anatomical compartments, including the liver, lungs, skin, and cardiovascular system; however, the impact of the exposome on other biological systems—such as the immune system—remains largely unexplored (Krutmann et al., 2017, Vasyutina et al., 2022; Gao and Snyder, 2021; Cheung et al., 2020).

In accordance with existing knowledge of the exposome and corresponding knowledge gaps within the scientific literature, the fundamental goal of this study was to develop an experimental animal model that could be used to evaluate biological responses to a common toxicant as a function of various exposomal influences. In order to investigate the role of the exposome in shaping workplace-associated health outcomes specifically, the model used in this study was designed to replicate a real-world occupational scenario relevant to the estimated 420,000 workers currently employed as welders full time in the United

States (Zeidler-Lrdely et al., 2012). Likewise, several exposomal factors associated with this occupation—consumption of an unhealthy diet, subchronic workplace respiratory exposures, and genetic influence—were incorporated into the model and investigated in vivo.

Briefly, 6-week-old rats were assigned to groups administered either a regular (Reg) or high fat (HF) diet for the entire 24 week study duration. After 7 weeks of maintenance on their respective diets, animals were then exposed to either filtered air or an occupationally-relevant dose of stainless steel welding fume (WF) via inhalation for 5 weeks, then allowed to recover for 12 additional weeks. A set of rats was sacrificed from each treatment group at three different time points representative of distinctive stages in the exposure/response timeline (before WF exposure, directly after, and following a 12 wk. recovery period) for collection of longitudinal health data. Although an extensive number of biological endpoints were assessed in this study, the results presented herein pertain specifically to the major alterations in local and systemic immune markers observed in the model (Antonini et al., 2019a; Antonini et al., 2019b; Boyce et al., 2020).

This study was conducted exclusively in male rats, consistent with knowledge that >95% of the welding workforce is male (Korczynski, 2000). To assess the impact of genetic variation on the immune parameters of interest in this model, two different rat strains were incorporated into the study. The Sprague-Dawley (SD) rat is a well-characterized outbred strain used extensively in biomedical research and has been frequently used in pulmonary toxicity studies and obesity models (Marques et al., 2016). Comparatively, the Brown Norway (BN) rat is an inbred strain predisposed to developing type 2 immune responses, IgE-mediated allergic reactivity, and autoimmunity (Kroese, 1998). The distinctive genetic backgrounds of these rats are known to contribute to well-documented discrepancies in immune, metabolic, and lung responses mounted by the two strains, and thus, their incorporation into this study was designed to mimic similar genetic variations seen in humans (Sáenz-Morales et al., 2010; Hall et al., 1997).

HF diet was selected as the behavioral/lifestyle component of the exposome in this study as large-scale shifts in eating patterns observed over the past century have been correlated to numerous health issues (Statovci et al., 2017). Moreover, consumption of a HF diet has been linked to immune dysfunction previously (Wasinski et al., 2013; Silva et al., 2020). To determine the influence of diet on various immune parameters in this study specifically, animals were fed a Reg or HF diet for the entire duration of the study. The HF diet used in this study was selected to be representative of a typical “Western diet,” and accordingly, was comprised of 14.8% protein, 40.6% carbohydrate, and 44.6% fat. Animals were maintained on this diet for 7 weeks prior to the WF exposure to replicate a real-world scenario in which an unhealthy eating pattern had been established prior to entering the workforce. This is consistent with studies that have demonstrated a propensity for unhealthy eating habits to develop in adolescence and persist through early life (Paeratakul et al., 2003). Studies have shown that children, teenagers, and young adults constitute the most frequent consumers of fast food and the greatest level of fat intake is generally seen in teenagers (Laroche et al., 2007; SD S, 2017).

One of the primary objectives in developing and implementing this in vivo model of the exposome was to determine if consumption of a HF diet has the capacity to alter immunological responsivity to a common respiratory toxicant. The study was also executed with the goal of identifying which experimental factor (genetics/strain, diet, occupational exposure) has the greatest capacity to modulate local and systemic markers of immune status and influence the severity and persistence of toxicant-induced pulmonary inflammation. The information obtained from these analyses will help elucidate which exposomic determinants may be particularly relevant in the context of immunotoxicity and occupational health, and accordingly, warrant special attention in future investigations. The results will also contribute to the development of other in vivo exposome models and direct future efforts to better understand the exposome and its impact on human health.

2. Materials and methods

2.1. Animals and die

Specific pathogen-free male SD (Hla: SD CVF; Hilltop Lab Animals, Scottdale, Pennsylvania) and BN (BN/RijHsd; Harlan Laboratories, Inc., Indianapolis, Indiana) rats (120 of each strain) were obtained at 5 weeks of age. Upon arrival, rats were provided tap water and irradiated Teklad 2918 regular diet (Reg; 18.6% protein, 44.2% carbohydrate, 6.2% fat; Envigo Teklad Diets, Madison, Wisconsin) ad libitum. All rats were *co*-housed in ventilated polycarbonate cages with HEPA-filtered air and maintained in a controlled humidity/temperature environment with a 12 h light/dark cycle in the AAALAC International-accredited National Institute for Occupational Safety and Health (NIOSH) Animal Facility.

After one week of acclimation, a set of animals from each strain (n = 60 rats/strain) was continued on the Reg Teklad 2918 diet or transitioned onto a Teklad Custom 45% Fat Kcal high-fat diet (HF; 14.8% protein, 40.6% carbohydrate, 44.6% fat; Envigo Teklad). The 45% Fat Kcal diet was designed with similarities to the western diet, and included the addition of 21% anhydrous milk fat, 34% sucrose, and 2% soybean for essential fatty acid supplementation. Animals were maintained on the Reg or HF diets and weighed at 4 week intervals until humanely euthanized with an intraperitoneal injection of sodium pentobarbital (> 100 mg/kg body weight; Fatal-Plus Solution, Vortech Pharmaceutical, Inc., Dcarborn, Michigan) and subsequent exsanguination via the abdominal aorta at the selected time points. All procedures in the studies comply with the ethical standards set forth by Animal Welfare Act and the Office of Laboratory Animal Welfare (OLAW). The studies were approved by the NIOSH Health Effects Laboratory Division (HELD) Institutional Animal Care and Use Committee within the Center for Disease Control and Prevention in accordance with an approved animal protocol (protocol number 18–004).

2.2. Experimental design and welding fume exposure

Beginning at 6 weeks of age, SD and BN rats were maintained on HF or Reg diets for 7 weeks (Fig. 1). Body weight was recorded for each animal every four weeks throughout the 24-week regimen. After the 7 weeks of diet maintenance, a set of rats from each strain was euthanized for collection of baseline parameters prior to WF exposure (7 wk. time point).

At the same time point, the remaining groups of rats were exposed by inhalation to stainless steel WF or filtered air (control) until week 12, at which time, half of the remaining animals from each strain were euthanized (12 wk. time point). Finally, the last set of SD and BN rats was allowed to recover from welding fume exposure for 12 weeks, and then euthanized (24 wk. time point). Following euthanasia, whole blood and serum were collected from each rat, bronchoalveolar lavage (BAL) was performed, and lymphoid tissues were harvested for subsequent analysis.

The design and construction of the welding fume aerosol generator and characterization of the fume used in this study have been previously described (Antonini et al., 2006; Antonini et al., 2011). Briefly, welding fume composition was determined by inductively coupled plasma-atomic emission spectroscopy according to NIOSH method 7300 and was composed of the following metals (weight %): Fe (53%), Cr (17%), Mn (24%), Ni (6%), and Cu (0.4%) (National Institute for Occupational Safety Health, 2003). Particle size distribution was determined in the exposure chamber within the breathing zone of the rats by using a Micro-Orifice Uniform Deposit Impactor (MOUDI, MSP Model 110, MSP Corporation, Shoreview, Minnesota) for general purpose aerosol sampling, and a Nano-MOUDI (MSP Model 115) that is specifically designed for sampling aerosols in the size range down to 0.010 μm. The mass median aerodynamic diameter was determined from a series of randomly-collected samples, measuring 0.26 μm with a geometric standard deviation of 1.4.

To accurately replicate a typical exposure scenario encountered by welders in the workplace, rats were exposed to an occupationally-relevant dose of WF via inhalation during weeks 7–12 of the study. Accordingly, animals in the WF treatment groups were exposed to a target fume concentration of 1200 mg/m^3 (20 mg/m^3 × 3 h/day × 4 days/week × 5 weeks)—a dose representative of 2–4 times that of the Threshold Limit Value (TLV, 5 mg/m^3) for a welder working an 8 h shift (Antonini et al., 2019b). The actual animal chamber concentrations (mean ± standard deviation) achieved during the exposures were 20.3 mg/m^3 ± 6.4 for the SD strain and 19.4 mg/m^3 ± 7.1 for the BN strain.

2.3. Phenotypic differentiation of circulating immune cell populations

Blood was drawn from the abdominal aorta directly following euthanasia by sodium pentobarbital overdose. A 500 μL aliquot of whole blood was separated from the total volume and collected into EDTA-coated vacutainers to prevent clotting and agitated continuously until analysis. Total leukocyte number was determined using an IDEXX Procyte Dx Hematology Analyzer (IDEXX Laboratories; Westbrook, ME). White blood cell subpopulations were also differentiated to determine absolute number and percentage of circulating monocytes, neutrophils, eosinophils, lymphocytes, and basophils.

2.4. Bronchoalveolar lavage

Following euthanasia, the trachea was cannulated and BAL was performed on rats to assess lung inflammation and retrieve immune cells present in the airway lumen. The lungs were lavaged with calcium- and magnesium-free PBS (pH 7.4) to yield a total of 30 mL of fluid, which was then centrifuged at 500 ×*g* for 10 min. Cell pellets from each BAL sample were washed and resuspended in 1 ml of PBS buffer. Cell suspensions were diluted into

isotonic buffer and used for enumeration of total BAL cell number, as well as size-specific population differentiation using a Coulter Multisizer II and AccuComp software (Coulter Electronics, Hialeah, Florida). Two separate aliquots, each containing 5.0×10^5 BAL cells, were retained for each sample for subsequent analysis by flow cytometry.

2.5. Collection and processing of spleens and lymph nodes

After the lungs of each animal were lavaged, the lung-associated lymph nodes were harvested and collected into sterile PBS. The spleen was also collected from each rat and sectioned into two halves—one half was placed directly into fixative solution for subsequent histopathological analysis and the other half was retained and placed in sterile PBS. Both lymphoid tissues were processed between frosted microscope slides to yield single cell suspensions in PBS. Cell concentrations were then evaluated in the lymph node samples using a Coulter Multisizer II (Coulter electronics; Hialeah, FL) to calculate total cell number for each animal.

2.6. Differentiation of immune cells in the lymph node, spleen, and BAL by flow cytometry

For phenotypic differentiation of immune cell subsets in the BAL, spleen, and lymph nodes, 5.0×10^5 cells form each sample were plated and suspended in FACS buffer (PBS + 1% bovine serum albumin +0.1% sodium azide) containing F_c receptor-blocking anti-rat CD32 (BD Biosciences). Cells were incubated for 5 min at 4 °C, washed, and resuspended in a staining solution containing a cocktail of fluorophore-conjugated antibodies. Two different staining panels were designed in order to differentiate immune cell subsets of lymphoid and myeloid origin. For each panel, a set of compensation controls was prepared using the respective cell type stained with a single fluorophore.

All three sample types were stained with the lymphocyte-differentiating panel. Lymph node, spleen, and BAL cells were stained with CD3-APC, CD4-BV421, CD8-BV605, CD44-FITC, CD45-PE-Cy7, CD45R (B220)-APC-Cy7, CD86-PE, and CD161-BV605 (BD Biosciences) to allow for identification of T-cells (CD45+/CD3+), CD4+ T-cells (CD45+/CD4+/CD8−), CD8+ T-cells (CD45+/CD4−/CD8+), B-cells (CD45+/CD45R+), and NK cells (CD45+/CD161+). Additionally, T-cell activation status was able to be evaluated in accordance with CD44 expression and B-cell activation was determined by CD86 expression levels. The gating strategy used to analyze cells in this staining panel is shown in Fig. S1.

The second aliquot of BAL cells was stained with the panel of antibodies to differentiate immune cells of myeloid origin. The panel contained CD11b-APC, CD43-AF647, CD45-PE-Cy7, CD68-PE, His48-FITC, and MHCII-PerCP (BD Biosciences), which allowed for differentiation of macrophages (CD45+/CD11b+/CD68+, high autofluorescence), neutrophils (CD45+/CD43+ high granularity), monocytes (CD45+/CD11b+/CD43+/His48+), and lymphocytes (CD45+/CD11b−/CD43−/His48−). In addition, MHC II expression level was used to determine macrophage activation status.

Cells were incubated in the corresponding staining cocktails for 30 min at 4 °C, washed, and resuspended in 100 μL Cytofix Buffer (BD Biosciences). After 20 min of incubation, the samples were washed and resuspended in FACS buffer, covered in foil, and stored at 4 °C until analysis. For each sample, 100,000 events were recorded on an LSR II

(BD Biosciences; San Diego, CA). In all analyses, doublet exclusion was performed (SSC-A vs SSC-H) and cell populations were gated using the FSC-A x SSC-A parameters for subsequent analysis. All data analyses were performed using FlowJo 7.6.5 Software (Treestar Inc.; Ashland, OR).

2.7. Statistical analysis

All statistical analyses were performed using GraphPad Prism version 7, JMP version 13, and SAS version 9.4 for Windows. Results from all studies are expressed as means ± standard error and considered statistically significant at $p < 0.05$.

Analyses of variance (ANOVAs) were performed within strain and time points for all variables. The 7 wk. time point utilized a one-way layout and the 12 and 24 wk. time points utilized a factorial two-way layout within each strain. For the 12 and 24 wk. analyses, post hoc pairwise comparisons among treatment groups were performed using the Fishers least significant difference test. For all analyses, a p value of <0.05 was set as the criterion for statistical significance.

Three-way ANOVAs were performed on the variables at each time point accounting for strain, exposure, diet, and all interactions to determine the proportion of variance attributed to each source of variation in the model. These analyses were based on the sum of squares (variation) for each source divided by the total sum of squares. These particular estimates are known as type III sums of squares and partition the variance from each source while all other sources were included in the model. Thus, if an interaction between exposure and diet takes up 25% of the variance, it means that there is 25% of the variance that cannot be accounted for by examining the main effects of exposure and diet by themselves. These analyses were performed on natural log-transformed data, as the data were generally distributed lognormally with a tail on the right, and thus heterogeneous variance. Only the sources of variance that were statistically significant were presented.

In addition, Principal Component Analysis (PCA) plots were used to simplify representation of multidimensional data and create weighted summation points for ease of visualization. PCA was performed on the variables and generated clustering for the primary variables and the principal components. The analyses were done for immune markers in a tissue-specific manner (lymph node, spleen, blood, BAL), as well as for all the data combined. Using a linear mathematical algorithm, a new set of variables (principal components) were derived that allowed us to highlight and visualize the differences between test group animals and variance among the animals in a group.

3. Results

3.1. Percent change in body weight

Animals were weighed throughout the duration of the study in order to monitor patterns of weight gain among the groups and identify potential associations between these trends and strain, diet, or WF exposure. As shown in Fig. 2, percent change in body weight was calculated (from corresponding baseline values at 0 wk) for each group every four weeks. Collectively, SD rats exhibited a greater capacity for weight gain throughout the course of

the study than the BN strain. SD rats gained an average of 252% of their baseline body weight by the 24 wk. time point, whereas this value was significantly lower in BN rats, at 137%.

In both SD and BN rats, HF diet consumption was associated with accelerated weight gain and greater maximal body weight change throughout the study; however, this trend was more pronounced in the BN strain. No significant differences in percent weight change were observed between BN groups maintained on the same diet at any time point (Fig. 2B), suggesting that in this strain, diet was the primary driver of discrepancies in weight gain between groups in the study. Comparatively, in SD rats, changes in body weight appeared to be dependent on both diet and WF exposure. Although both HF groups exhibited consistent changes in body weight throughout the study, SD rats maintained on the Reg diet did not. Most notably, WF exposure appeared to induce a suppressive effect on weight gain in SD rats of the Reg/WF group—an effect which persisted until the end of the study.

3.2. Phenotypic analysis of immune cell subsets within the bal

Following euthanasia, the lungs of each animal were lavaged. The cells obtained front this technique were then analyzed to evaluate local inflammatory responses within the airways. The total number of cells retrieved from the lungs of SD and BN rats by BAL was determined first and is depicted in Fig. 3. At 12 wks, total BAL cell number was significantly elevated in all WF-exposed groups. This response did not appear to be influenced by diet, as no differences were observed between HF/WF and Reg/WF group values within either strain. In SD rats, BAL cell counts returned to baseline levels in both WF-exposed groups by 24 wks. In contrast, cell number remained significantly and consistently elevated in both WF-exposed groups of BN rats at 24 wks.

Although diet did not appear to impact total BAL cell number at any time point in either strain of rat, differentiation of BAL cell subsets by flow cytometry revealed that HF diet was associated with modulation of the BAL phenotypic profile in both SD and BN rats following WF exposure. In SD rats exposed to WF, similar increases in BAL macrophage activation status (evaluated by MHCII expression level) were observed between the HF and Reg groups at 12 wks; however, alveolar macrophages constituted a significantly lower proportion of total BAL cells in the HF group (50.1% compared to 73.3% in Reg/WF group). This observation remained evident until the end of the study. At 24 wks, BAL macrophage proportionality returned to baseline levels in the Reg/WF group (~92%) but remained significantly decreased in the HF/WF group (77.4%).

Comparatively, the alveolar macrophage compartment was differentially augmented in response to HF diet and WF exposure in BN rats. WF exposure caused a signfiicant decrease in the proportion of BAL macrophages at 12 wks, but the magnitude of this response was conserved between both groups of BN rats. Despite similarities in total macrophage number and proportion between the groups, animals maintained on the HF diet exhibited a significantly increased ratio of activated macrophages compared to rats fed the Reg diet (31.2% compared to 17.5%). This discrepancy was attenuated by the 24 wk. time point, although percent BAL macrophage activation remained elevated in both WF groups (9.6–8.5%) and the HF/air group (5.1%) compared to Reg/air animals (1.6%). At this time point,

the percentage of alveolar macrophages within the BAL of both WF-exposed groups of BN rats remained decreased over air-exposed animals, yet became significantly different with respect to diet. In the HF/WF group, the percent of BAL macrophages continued to decrease after 12 wks, reaching a value of 70.2% at 24 wks. In the Reg/WF group, macrophage proportionality increasedly modestly during the recovery period, representing 83.4% of BAL cells by 24 wks.

WF exposure was associated with an increase in the number and proportion of lymphocytes within the BAL of SD and BN rats at 12 wks. In both strains, these values were significanly higher in the HF group compared to the Reg group (Fig. 4). At 24 wks, BAL lymphocytes remained significantly elevated exclusively in the HF/WF group of SD rats. In BN rats, BAL lymphocyte number remained significantly elevated in both the HF/WF and Reg/WF groups at 24 wks; however, the proportionality of lymphocytes comprising the total pool of BAL cells was only significantly elevated in the HF/WF group at this time point.

WF exposure also led to significant increases in BAL neutrophils in both rat strains at 12 wks. Absolute number and proportionality of neutrophils was higher in the HF/WF group of SD rats compared to the Reg/WF group at this time point. The opposite effect was observed in BN rats, as the greatest increase in neutrophils was seen in the Reg/WF group at 12 wks. Similar to the animals' BAL lymphocyte respsonses, BAL neutrophil number and population ratio remained elevated only in the HF/WF group of SD rats at 24 wks. Both the total number and percentage of BAL neutrophils remained significantly increased in both WF-exposed groups of BN rats at 24 wks; however, the magnitude of this increase was greatest in the HF/WF group with respect to both parameters.

3.3. Lymph node cellularity and differentiation of immune cell subsets

The mediastinal lymph nodes were collected from each animal at all time points to evaluate local inflammatory responses in the airways and assess corresponding immunological activity in lymphoid tissues associated with the respiratory tract. Lymph node cellularity was evaluated first by quantifying the total number of cells comprising the nodes in each animal. Baseline measurements of lymph node cellularity did not differ significantly between groups maintained on either diet, irrespective of strain, at the 7 wk. time point (Figs. 5 and 6). All groups subsequently exposed to WF exhibited increases in lymph node size at 12 wks compared to air-exposed animals of the same strain. In SD rats, total cell number was further elevated in the group maintained on the IIF diet compared to those administered regular chow—an effect not observed in BN rats. Significant increases in lymph node cellularity were still evident in HF/WF groups of both strains at 24 wks, as well as in WF-exposed SD rats maintained on the regular diet.

Phenotypic analysis was then performed to characterize the cellular composition of the lymph nodes in each animal of the study. Accordingly, it was determined that administration of the HF diet was associated with a few notable alterations in the cellular profile of the lymph nodes in both strains at the 7 wk. time point (Figs. 5 and 6). More pronounced effects were observed in the SD strain, wherein HF diet led to a decreased percentage of T-lymphocytes and increased B-cell prevalence, ultimately causing an increase in the B:T ratio within the nodes (0.34 compared to 0.23 in Reg animals). In BN rats, administration

of the HF diet for 7 weeks only caused alterations in the B-cell compartment of the nodes. At 7 wks, an increase in the overall prevalence of B-cells was observed (22.9% compared to 16.9%) within the lymph nodes and a greater percentage of activated cells within this population was also observed (11.8% compared to 3.8%).

At 12 wks, WF exposure was associated with significant increases in lymphocyte activation within the lymph nodes of SD rats; however, the proportionality of lymphocyte subsets within the nodes remained largely consistent between the HF/air, Reg/WF, and Reg/air groups. In the HF/WF group, the alterations in cellular constituents of the nodes observed at 7 wks became more pronounced at the 12 wk. time point. These animals exhibited a considerably greater proportion of B-cells and significantly fewer T-cells than all other groups at the same time point, further elevating the B:T ratio in these animals (0.53). A greater degree of cellular activation was also evident in the CD8+ T-cell and B-cell subpopulations of lymphocytes within the nodes of SD rats of the HF/WF group at 12 wks.

BN rats exhibited similar trends in lymph node cell phenotypic alterations at 12 wks as those observed in SD rats following WF exposure. Lymphocyte subset ratios remained largely conserved between the HF/air, Reg/WF, Reg/air groups, although greater numbers of activated lymphocytes were observed in the Reg/WF group compared to air-exposed groups. A similar increase in lymphocyte activation was also seen in the HF/WF group. The nodes of these animals exhibited a decreased number of CD8+ T-cells and a greater proportion of B cells when compared to all other groups at 12 wks. As a result, the lymph node CD+:8 T-cell ratio became significantly elevated in animals in the HF/WF group (18.7 compared to 9.8–12.9) at this time point.

At the 24 wk. time point, WF-induced alterations in the lymph node phenotypic profile returned to baseline values in the Reg diet-fed groups of both strains. In contrast, the majority of the population shifts observed following exposure persisted up to the final time point in the HF groups. Furthermore, the percent of cells expressing an activated phenotype remained significantly increased for all three lymphocyte populations in the nodes of the HF/WF groups of both strains.

3.4. Phenotypic analysis of immune cell subsets within the spleen

The spleens were harvested from each animal in the study and subjected to similar phenotypic analyses as those performed on the lymph nodes in order to evaluate systemic immune alterations associated with strain, diet, and exposure (Fig. 7). Accordingly, the only notable change in lymphocyte subset proportionality at the 7 wk. time point was observed in SD rats, wherein the HF group exhibited a decreased percentage of non-lymphoid cells occupying the spleen (13.4% of all cells, compared to 18.5% in Reg animals).

At 12 wks, both IIF diet-fed groups of the 3D strain exhibited an increased proportion of lymphoid cells within the spleen and lower numbers of non-lymphoid cells compared to air-exposed groups (Fig. 7). Within the splenic lymphocyte pool, a decreased percentage of total T-cells and CD4+ subsets was seen in all groups maintained on either the HF diet or exposed to WF when compared to the Reg/air group. Although no significant differences in CD8+ T-cell proportionality were observed between any groups, an elevated percentage

of activated cells within this subpopulation was observed in the WF-exposed groups at 12 wks—the magnitude of which was dependent on diet. The proportion of B-cells (and B:T ratio) within the spleen was also elevated in the HF/WF, HF/air, and Reg/WF groups at 12 wks; however, the greatest increase was observed in the HF-fed SD rats, irrespective of WF/air exposure. Despite the increased number of splenic B-cells in all three groups, significant increases in B-cell activation were only seen in the HF/WF group at 12 wks.

Unlike in SD rats, alterations in the proportionality of splenic lymphoid and non-lymphoid cell populations in BN rats at 12 wks appeared conserved with respect to exposure. WF-exposed groups exhibited higher numbers of lymphocytes within the spleen and fewer non-lymphoid cells when compared to air-exposed BN rats at the same time point. Despite this discrepancy, alterations in the splenic lymphocyte pool of BN rats exhibited similar trends as those seen in SD rats at 12 wks. T-cell proportionality declined in both WF-exposed groups and the magnitude of B-cell expansion increased, leading to significant elevations in the spleen B:T ratio of these groups. An observation unique to the BN strain was the significant decrease in CD4:8 ratio within the spleens of WF-exposed animals (4.7 and 4.9 compared to 5.6 and 5.8 in air groups) at this time point.

By 24 wks, the only significant alterations in splenic lymphocyte population ratios observed in both SD and BN rats were exclusively seen in the HF/WF groups. The decrease in T-cell prevalence and elevated B-cell frequency within the spleen persisted in these animals, and notable increases in lymphocyte activation were also still evident at the final time point of the study. In addition, a rise in the percent of activated B-cells reached significance in the HF/air group of BN rats by 24 wks.

3.5. Circulating leukocyte populations

Whole blood was collected from each animal to evaluate any alterations in the circulating leukocyte profile throughout the study. First, total blood leukocyte number was determined. Likewise, at 7 wks, diet-induced alterations in total blood leukocyte number were evident in both strains, however, HF diet was associated with divergent effects between SD and BN rats (Figs. 8 and 9). In the SD strain, administration of the HF diet led to decreased numbers of circulating immune cells (4.63 K cells/μL blood compared to 5.90 in the Reg group), whereas the HF group of BN rats exhibited elevated total blood leukocyte numbers over Reg animals (7.98 K/μL compared to 6.56). Interestingly, these trends were no longer evident at the 12 wk. time point. Following 5 wks of WF exposure, total blood leukocytes were greatest in the HF/WF group of the SD strain and the Reg/air group of BN rats. After the 12 wk. recovery period, the only notable discrepancy in total blood leukocyte number was a decrease observed in the HF-fed BN rats (3.89–4.63 K/μL) when compared to the Reg groups at 24wk (5.24–5.75).

In addition to quantifying the total number of circulating leukocytes, subsets of immune cells were also differentiated in order to identify any discrepancies in absolute number or proportionality of specific leukocyte subpopulations present in the blood during the course of the study. At 7wk, diet-induced alterations in the blood immune cell profile were only evident in SD rats. SD rats administered the HF diet had an elevated number and proportion of blood neutrophils compared to rats fed the Reg diet. As shown in Fig. 10, expansion of

this subpopulation was accompanied by a concurrent decrease in blood lymphocyte burden. Despite alterations in total blood leukocyte number in BN rats at the same time point, HF diet did not impact the proportionality of any cell subpopulations in this strain at 7 wks.

Although total leukocyte number was exclusively increased in the HF/WF group of SD rats at 12 wks, alterations in blood neutrophil and lymphocyte populations appeared conserved between groups with respect to diet, irrespective of WF exposure. HF groups exhibited a greater proportion of circulating neutrophils and a lower ratio of lymphocytes compared to the Reg groups. By comparison, blood neutrophil and lymphocyte populations in BN rats at 12 wks were similarly altered among groups with respect to pulmonary exposure, irrespective of diet—an association that became more pronounced by the 24 wk. time point. WF exposure led to a higher percentage of blood neutrophils in BN rats at this time point, while lymphocytes represented a less prevalent subset within the total leukocyte pool. In contrast, most of the alterations in circulating immune cell populations observed in SD rats at previous time points had normalized after the recovery period, returning to baseline values by 24 wks.

3.6. Proportion of variance and PCA

To evaluate the overarching impact of strain, exposure, and diet (and corresponding interactions between these variables) on the immune responses observed in this study, PCA analysis was performed. A proportion of variance was determined by assessing 3-way ANOVAs on the variables at each time point to determine which experimental factor contributed with greatest significance to a particular immunological endpoint. As shown in Fig. 11, the analyses were first performed in the context of tissue-specific (BAL, lymph node, spleen, blood) immune markers.

In Fig. 11a, a PCA plot generated using BAL-specific parameters is shown. The variable most prominently associated with the clustering pattern of lung associated immune markers in this study was exposure (WF vs air). A clear separation between air- and WF-exposed animals is evident on the PCA plot, irrespective of strain, diet, or time. Diet was the second most influential variable with respect to lung immune markers in the study. The capacity for WF-exposed animals to recover to BAL baseline values by 24 wks was dependent on diet, whereby rats fed the regular diet recovered and those fed the HF diet did not. Finally, strain was also determined to be influential in BAL responses, albeit to a lesser degree than exposure or diet. Most notably, in WF-exposed animals, the BN strain exhibited a slower propensity for recovery over the SD strain.

The PCA plot generated from lymph node-specific endpoints is shown is Fig. 11b. From the analysis, it was determined that strain was the primary driving factor in the clustering of lymph node-associated immune endpoints. Accordingly, a clear separation between all points representative of SD (blue points) and BN (orange points, responses is evident on the plot. Diet and exposure were the second most influential variables with respect to lymph node parameters, followed by recovery time. Comparatively, in the spleen, clustering of tissue-specific endpoints (Fig. 11c) determined by PCA only became apparent after WF exposure at 12 wks—an effect which was dependent on strain, and to a lesser degree, diet. Finally, for PCA of blood-specific parameters (Fig. 11d), all endpoints considered in this

analysis exhibited minimal differentiation, irrespective of strain, diet, exposure, or recovery time. Although some general trends were observed, the variables were all weakly correlated.

A summary PCA plot incorporating all immune parameters measured in the study (BAL, lymph node, spleen, and blood markers) is shown in Fig. 12. From this analysis, it can be inferred that the collective immune responses observed in the study were most critically dependent on strain, as illustrated by the clear separation of SD (blue points) and BN (orange points) groups on the plot. Overall, baseline controls and air-exposed groups remained clustered together throughout the study. At 12 wks, responses tended to cluster in an exposure-dependent manner with respect to strain. By 24 wks, recovery from WF exposure was shown to be dependent on both strain and diet. In SD rats, WF-exposed animals recovered completely if fed the regular diet, while those fed the HF diet remained separated from the other groups at 24 wks on the PCA plot. In BN rats, both WF-exposed groups failed to recover completely by 24 wks; however, animals administered the regular diet exhibited a greater propensity for recovery over those fed the HF diet.

4. Discussion

The goal of this study was to utilize an in vivo model of the exposome that was designed to mimic a real-world occupational scenario to collect longitudinal health data, and subsequently, determine the impact of genetics and diet on biological responses following subchronic respiratory toxicant exposure Findings from the study demonstrated that behavioral/lifestyle factors (represented by HF diet) can not only directly influence baseline immune status, but also subsequent responses to inflammatory insults like WF inhalation. These alterations could be detected both locally and on the systemic level following toxicant exposure. Moreover, results indicated that genetic influences (represented by variations in rat strain) are one of the fundamental contributors to the immune response and its susceptibility to augmentation by lifestyle factors, such as consumption of a HF diet.

One of the most notable findings from this study was that several significant alterations in various immune parameters were observed in both rat strains at 7 wks, indicating that HF diet alone was capable of modulating systemic immune status. The most pronounced alterations were observed in the lung-associated lymph nodes (increased B-cell and decreased T-cell proportionality, greater activation of B-cells) and blood (increased circulating leukocyte number). Overall, these changes were more prominently observed in SD rats compared to BN rats. The propensity for HF diet to augment various immune markers at 7 wks in this study is consistent with other reports of the effects of a Western diet on the immune system (Pongratz et al., 2015). Previous studies in mice have shown that similar alterations in lymphocyte populations within various compartments of the immune system following HF diet result from significantly acceleated rates of hemaotpoesis and lymphopoesis (Trottier et al., 2012; Götz et al., 2011). HF diet has also been shown to augment numbers of innate and adaptive immune cells in the blood and various tissues in rats, induce gut dysbiosis, modulate neutrophil activities, and mediate polarization of macrophages towards a pro-inflammatory M1 state—all of which can mediate profound impacts on immune system functionality (Butler, 2021; Malesza et al., 2021; Kiran et al., 2022; Moorthy et al., 2016). Many of these diet-induced immune alterations likely underlie

observations that consumption of the Western diet increases the risk of developing diabetes, autoimmune disease, respiratory and contact allergy, and other inflammatory conditions (Silva et al., 2020; Manzel et al., 2014; Rühl-Muth et al., 2021).

At 12 wks, both rat strains exhibited prototypical markers of acute airway inflammation in response to WF exposure, including elevated lactate dehydrogenase (LDH) levels (data shown in Antonini *et. al*, 2019), increased total BAL cell and neutrophil number, enhanced activation of alveolar macrophages, and alterations in lung-associated lymph node cell subset proportionality (Anderson et al., 2007). In general, HF diet appeared to preferentially impact the inflammatory response to WF in SD rats. At 12 wks, several of the immune marker alterations caused by the exposure differed in magnitude between the HF/WF and Reg/WF groups (lymph node size, total circulating leukocyte count, BAL macrophage proportionality). This discrepancy is consistent with earlier observations indicating enhanced immune responsivity to HF diet in this strain (altered lung-associated lymph node, spleen, and blood immune cell population ratios at 7 wks). It has been suggested that the low-level systemic inflammation induced by HF can prime the airways for inflammatory insult by lowering the threshold of exposure required to trigger innate immune activation and amplifying early inflammatory mechanisms (Suratt, 2016). Concurrently, this heightened state of immunological responsiveness has been implicated in an accelerated transition into the subsequent resolution phase of lung injury. The responses observed in the SD rats of this study appear consistent with this mechanism, as those maintained on the HF diet exhibited a greater ability to recover from local inflammation caused by WF exposure. At 24 wks, total cell number, neutrophil number, and LDH in the BAL of SD HF/WF animals had all returned to baseline values.

In contrast, the effects of HF diet appeared more influential on the capacity for immune recovery and long-term effects of WF exposure in BN rats. At 12 wks, most immune parameter changes were conserved between BN groups with respect to exposure (blood neutrophils and lymphocytes, BAL macrophage proportionality); however, following the recovery period, several diet-associated discrepancies emerged between the HF/WF and Reg/WF groups (circulating leukocyte number, spleen cell populations, BAL macrophage proportionality) by 24 wks. HF diet was responsible for prolonged elevations in total lymph node cell number, BAL lymphocyte number, and lymphocyte activation status compared to Reg diet-fed animals exposed to WF. Overall, BN rats exhibited a compromised capacity for resolution of WF-induced inflammation when compared to SD rats. Local inflammation was still evident within the airways of WF-exposed animals at 24wk, as significantly elevated total cell numbers, neutrophil counts, and LDH levels were detected in the BAL of both HF/WF and Reg/WF groups at this time point.

In both strains, significant numbers of activated lymphocytes were still evident in the lung-associated lymph nodes and spleens of WF-exposed animals fed the HF diet at the final time point. The proportion of activated alveolar macrophages remained elevated in these groups at 24 wks, as well. Interestingly, a few similar increases in immune cell activation, independent of WF exposure, were obervsed exclusively in the BN strain. At 24 wks, a higher percentage of lung-associated lymph node and splenic B-cells, as well as BAL macrophages, expressed elevated levels of activation markers in the

HF/air group. Collectively, these findings imply that HF diet is capable of disrupting the normal mechanisms responsible for attenuating heightened immunological responsivity after toxicant exposure in both strains; however, BN rats were preferentially susceptible to HF-induced immune alterations in the absence of such insult.

The endpoints of interest in this study were selected as preliminary indicators of the animals' susceptibility to HF diet-induced alterations in immune responsivity. Although many of the measured parameters exhibited associations with exposomal factors, the functional implications of these findings remain unclear and are beyond the scope of the present study. Additional studies are required in order to determine whether the observed effects are capable of mediating clinically-significant immunomodulatory responses, such as the development of allergy or autoimmunity. The impact of each exposomal factor can also be explored in greater depth in future studies to elucidate individual variable effects on specific immune cell subsets, lymphoid tissues, or functional compartments of the immune system (e.g., innate immune activity, cell-mediated or humoral processes), as well as the underlying mechanisms responsible for these alterations. Although this study was able to identify a few specific exposomal factors capable of influencing immune responses, countless other influences could be analyzed in future studies and used to help advance our understanding of the exposome. Most notably, the inclusion of both male and female rats could help discern any sex-specific exposomal influences. The introduction of a pre-existing co-morbidity, such as asthma or obesity, could also be incorporated into future models. Other increasingly relevant exposomal factors might include environmental co-exposures (e.g., cigarette smoke or air pollution), sleep deprivation or microbial infection.

Overall, the findings of this study are consistent with outer observations reported within the growing body of scientific literature on the exposonte and emphasize the potential significance of many frequently-overlooked contributors to human health and disease. Our results demonstrated, most notably, that the initial severity of WF-induced subchronic lung injury and the subsequent resolution of inflammation is directly impacted by multiple exposomal factors—in this case, genetics and diet, specifically. As it becomes increasingly evident that most biological processes and adverse health effects are subject to profound influence from various external and internal forces, the role of the exposonte in human health and disease is likely to garner additional scientific attention in the coming years. Subsequent advances in our understanding of the exposonte can then be applied to improve health outcomes in both the general public and workers by facilitating significant improvements in our capacity to identify individuals and populations at increased risk for disease development, prevent the initiation and progression of early pathogenic processes, and effectively manage disease activity in afflicted subjects.

Supplementary Material

Refer to Web version on PubMed Central for supplementary material.

Acknowledgments

The authors would like to acknowledge Bared L. Cumpston, Howard D. Leonard, James B. Cumpston, and the rest of the NIOSH Morgantown inhalation exposure team for their contributions to this study.

Funding

This work was funded through the NIOSH National Occupational Research Agenda (project 927ZLEG).

Data availability

Data will be made available on request.

Abbreviations:

BAL	bronchoalveolar lavage
BN	Brown Norway
HF	high fat diet
Reg	regular diet
LDH	lactate dehydrogenase
PCA	principal components analysis
SD	Sprague-Dawley
Th	helper T-cell
TLV	threshold limit value
WF	welding fume

References

Anderson SE, Meade BJ, Butterworth LF, Munson AE, 2007 The humoral immune response of mice exposed to manual metal are stainless steel-welding fumes. J. Immunotoxicol 4 (1), 15–23. [PubMed: 18958709]

Antonini JM, Afshari AA, Stone S, Chen B, Schwegler-Berry D, Fletcher WG, et al., 2006. Design, Construction, and Characterization of a Novel Robotic Welding Fume Generator and Inhalation Exposure System for Laboratory Animals, 3(4), pp. 194–203.

Antonini JM, Keane M, Chen BT, Stone S, Roberts JR, Schwegler-Berry D, et al., 2011. Alterations in Welding Process Voltage Affect the Generation of Ultrafine Particles, Fume Composition, and Pulmonary Toxicity., 5(4), pp. 700–710.

Antonini JM, Kodali V, Meighan TG, Roach KA, Roberts JR, Salmen R, et al. , 2019a. Effect of age, high-fat diet, and rat strain on serum biomarkers and telomere length and global DNA methylation in peripheral blood mononuclear cells. Sci. Rep 9 (1), 1996. [PubMed: 30760804]

Antonini JM, Kodali V, Shoeb M, Kashon M, Roach KA, Bosce G, et al. , 2019b. Effect of a high fat diet and occupational exposure in different rat strains on lung and systemic responses: examination of the exposome in an animal model. Toxicol. Sci 9 (1996), 1–9.

Boyce GR, Shoeb M, Kodali V, Meighan TG, Roach KA, McKinney W, et al. , 2020. Welding fume inhalation exposure and high-fat diet change lipid homeostasis in rat liver. Toxicol. Rep 7, 1350–1355. [PubMed: 33102138]

Butler MJ, 2021. The role of Western diets and obesity in peripheral immune cell recruitment and inflammation in the central nervous system. Brain Behav. Immun. Health 16, 100298. [PubMed: 34589790]

Carlsten C, 2018. Synergistic environmental exposures and the airways capturing complexity in humans: an underappreciated world of complex exposures. Chest. 154 (4), 918–924. [PubMed: 29909283]

Cheung AC, Walker DI, Juran BD, Miller GW, Lazaridis KN, 2020. Studying the exposome to understand the environmental determinants of complex liver diseases. Hepatology (Baltimore, Md). 71 (1), 352.

Fang M, Hu L, Chen D, Guo Y, Liu J, Ian C, et al. , 2021. Exposome in human health: utopia or wonderland? Innovation. 2 (4), 100172. [PubMed: 34746906]

Gao P, Snyder M, 2021. Exposome-wide association study for metabolic syndrome. Front. Genet 12, 783930. [PubMed: 34950191]

Götz AA, Rozman J, Rodel HG, Fuchs H, Gailus-Durner V, de Angelis MH, et al. , 2011. Comparison of particle-exposure triggered pulmonary and systemic inflammation in mice fed with three different diets. Partic. Fibre Toxicol 8 (1), 30.

Hall E, Parton R, Wardlaw AC, 1997. Differences in coughing and other responses to intrabronchial infection with Bordetella pertussis among strains of rats. Infect. Immun 65 (11), 4711–4717. [PubMed: 9353055]

Kiran S, Rakib A, Kodidela S, Kumar S, Singh UP, 2022. High-fat diet-induced dysregulation of immune cells correlates with macrophage phenotypes and chronic inflammation in adipose tissue. Cells 11 (8).

Korczynski R, 2000. Occupational health concerns in the welding industry. Appl. Occup. Environ. Hyg 15 (12), 936–945. [PubMed: 11141606]

Kroese F, 1998. Immunology of the Rat, Handbook of Vertebrate Immunology. Academic, London (p. 137).

Krutmann J, Bouloc A, Sore G, Bernard BA, Passeron T, 2017. The skin aging exposome. J. Dermatol. Sci 85 (3), 152–161. [PubMed: 27720464]

Laroche HH, Hofer TP, Davis MM, 2007. Adult fat intake associated with the presence of children in households: findings from NHANES III. J. Am. Board Fam. Med 20 (1), 9–15. [PubMed: 17204729]

Malesza IJ, Malesza M, Walkowiak J, Mussin N, Walkowiak D, Aringazina R, et al. , 2021. High-fat, Western-style diet, systemic inflammation, and gut microbiota: a narrative review. Cells. 10 (11), 3164. [PubMed: 34831387]

Manzel A, Muller DN, Hafler DA, Erdman SE, Linker RA, Kleinewietfeld M, 2014. Role of “Western diet” in inflammatory autoimmune diseases. Curr Allergy Asthma Rep 14 (1), 404. [PubMed: 24338487]

Marques C, Meireles M, Norberto S, Leite J, Freitas J, Pestana D, et al. , 2016. High-fat diet-induced obesity rat model: a comparison between Wistar and Sprague-Dawley rat. Adipocyte. 5 (1), 11–21. [PubMed: 27144092]

Martin-Sanchez F, Bellazzi R, Casella V, Dixon W, Lopez-Campos G, Peek N, 2020. Progress in characterizing the human exposome: a key step for precision medicine. Yearb. Med. Inform 29 (1), 115–120. [PubMed: 32303099]

Moorthy AN, Tan KB, Wang S, Narasaraju T, Chow VT, et al., 2016. Front. Immunol 7, 289. [PubMed: 27531997]

National Institute for Occupational Safety Health, 2003. Method 7300, Elements by ICP. NIOSH Manual of Analytical Methods. US Department of Health and Human Services Centers for Disease Control and Prevention.

Paeratakul S, Ferdinand DP, Champagne CM, Ryan DH, Bray GA, 2003. Fast-food consumption among US adults and children: dietary and nutrient intake profile. J. Am. Diet. Assoc 103 (10), 1332–1338. [PubMed: 14520253]

Pongratz G, Lowin T, Kob R, Buettner R, Bertsch T, Bollheimer LCJI, et al., 2015. A Sustained High Fat Diet for Two Years Decreases IgM and IL-1 Beta in Ageing Wistar Rats, 12(1), pp. 1–9.

Robinson O, Vrijheid M, 2015. The pregnancy exposome. Curr. Environ. Health Repor 2 (2), 204–213.

Rühl-Muth AC, Maler MD, Esser PR, Martin SF, 2021. Feeding of a fat-enriched diet causes the loss of resistance to contact hypersensitivity. Contact Dermatitis 85 (4), 398–406. [PubMed: 34218443]

Sáenz-Morales D, Conde E, Blanco-Sánchez I, Ponte B, Aguado-Fraile E, de Las, Casas G, et al. , 2010. Differential resolution of inflammation and recovery after renal ischemia–reperfusion injury in Brown Norway compared with Sprague Dawley rats. Kidney Int. 77 (9), 781–793. [PubMed: 20164827]

SD S, 2017. Junk Food Consumption Among Secondary Level Students, Chitwan. J. Nepal Paediat. Soc 37 (2).

Silva FmdCe, Oliveira EEd, Ambrósio MGE, Ayupe MC, Souza VPD, Gameiro J, et al. , 2020. High-fat diet-induced obesity worsens TH2 immune response and immunopathologic characteristics in murine model of eosinophilic oesophagitis. Clin. Exp. Allergy 50 (2), 244–255. [PubMed: 31837231]

Statovci D, Aguilera M, MacSharry J, Melgar S, 2017. The impact of western diet and nutrients on the microbiota and immune response at mucosal interfaces. Front. Immunol 8, 838. [PubMed: 28804483]

Suratt BT, 2016. Mouse modeling of obese lung disease. Insights and caveats. Am. J. Respir. Cell Mol. Biol 55 (2), 153–158. [PubMed: 27163945]

Trottier MD, Naaz A, Li Y, Fraker PJ JPotNAoS, 2012. Enhancement of Hematopoiesis and Lymphopoiesis in Diet-induced Obese Mice, 109(20), pp. 7622–7629.

Vasyutina M, Alieva A, Reutova O, Bakaleiko V, Murashova L, Dyachuk V, et al. , 2022. The zebrafish model system for dyslipidemia and atherosclerosis research: focus on environmental/exposome factors and genetic mechanisms. Metabolism. 129, 155138. [PubMed: 35051509]

Wasinski F, Bacurau RF, Moraes MR, Haro AS, Moraes-Vieira PM, Estrela GR, et al. , 2013. Exercise and caloric restriction alter the immune system of mice submitted to a high-fat diet. Mediat. Inflamm 2013.

Wild CP, 2005. Complementing the Genome with an “Exposome”: The Outstanding Challenge of Environmental Exposure Measurement in Molecular Epidemiology. AACR.

Zeidler-Erdely PC, Erdely A, Antonini JM, 2012. Immunotoxicology of are welding fume: worker and experimental animal studies. J. Immunotoxicol 9 (4), 411–425. [PubMed: 22734811]

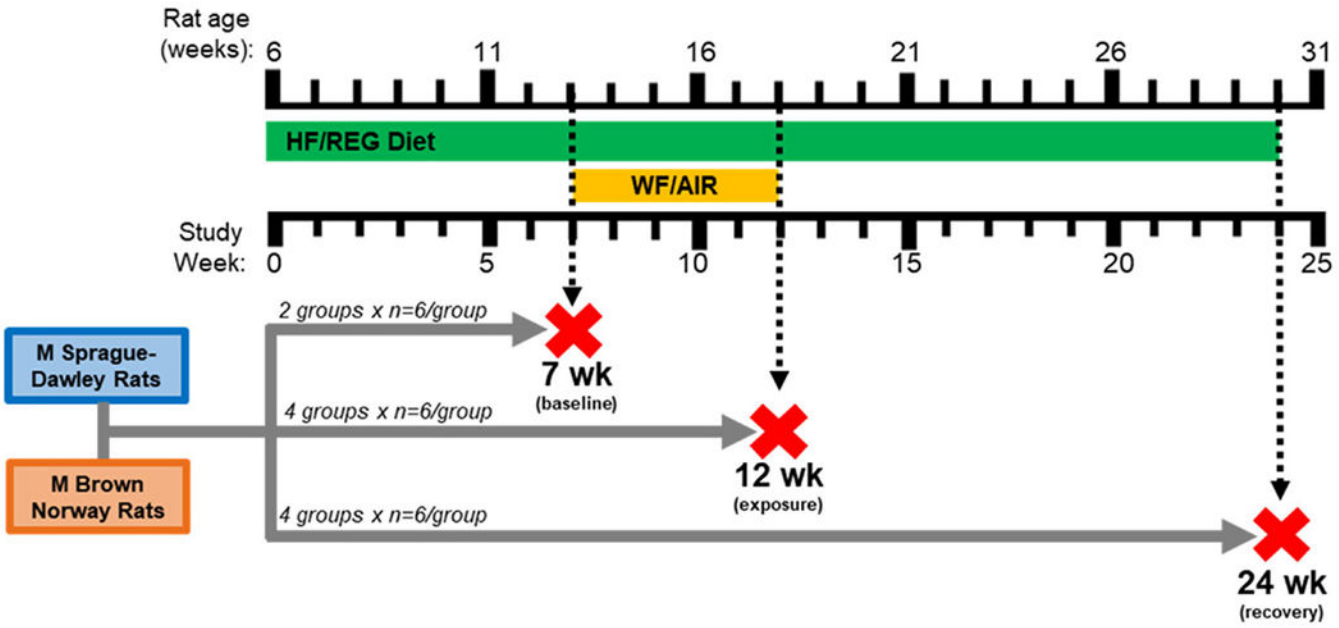

Fig. 1.

Experimental design and schedule of exposures. At 6 weeks of age, male Sprague-Dawley and Brown Norway rats were started on either regular (Reg) or high fat (HF) diets (week 0). After 7 weeks of diet maintenance, a set of animals (n = 6/group) was sacrificed from each strain to acquire baseline data (7 wk. time point). The remaining animals were continued on the respective diets and subsequently exposed to air or welding fumes (WF, 20 mg/m^3 x 3 h/day x 20 days) from weeks 7 to 12. One set of animals (n = 6/group) was euthanized from each strain in order to acquire post-exposure immune parameters (12 wk. time point). Finally, the last group from each strain was maintained on the same diet regimen and allowed to recover from the previous exposure for 12 weeks. The final groups (n = 6/group) were euthanized at the 24 wk. time point and immune endpoints were evaluated for the recovery phase. (For interpretation of the references to colour in this figure legend, the reader is referred to the web version of this article.)

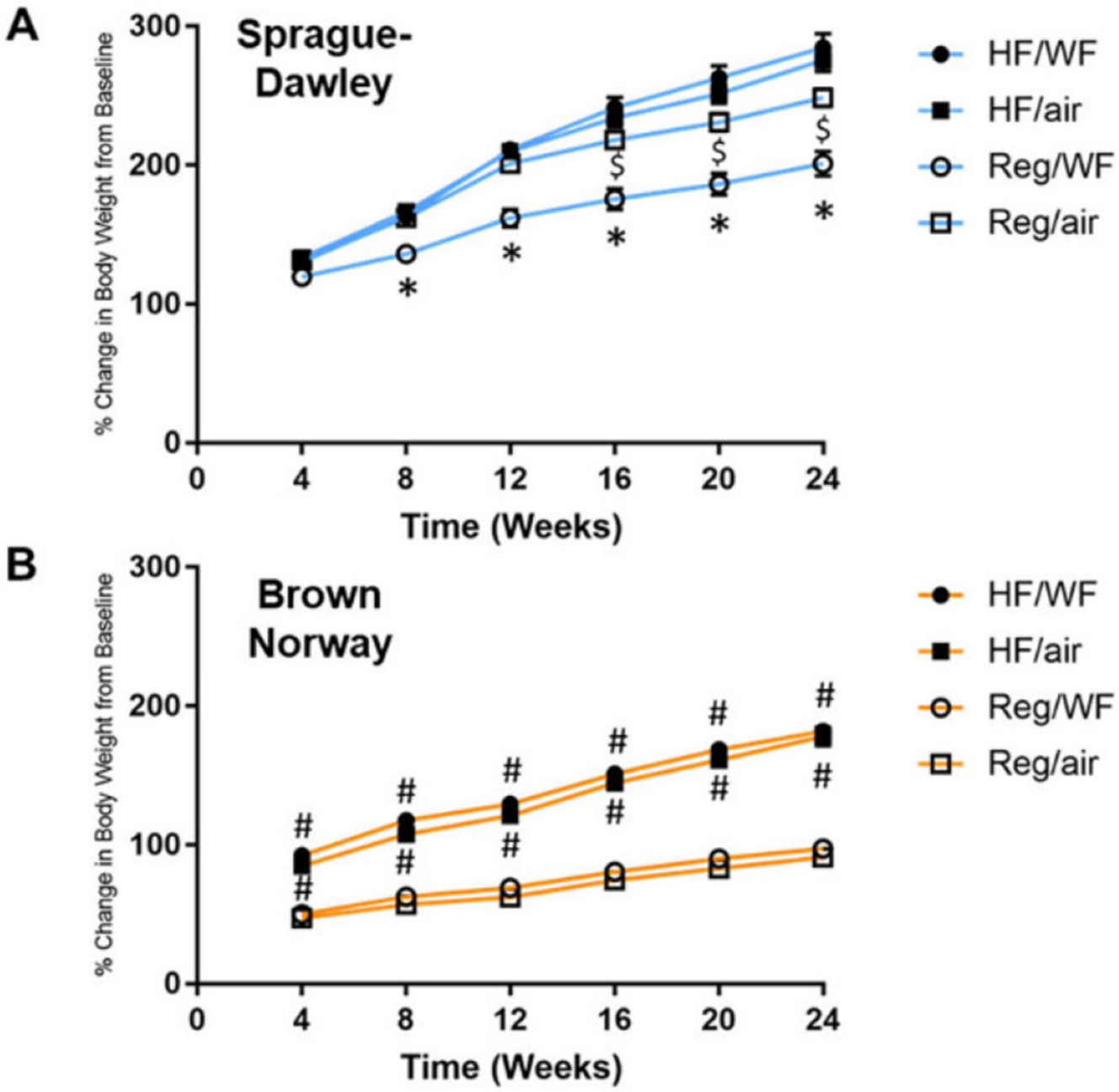

Fig. 2.

Changes in animal body weights over the course of the 24 week study. Using baseline values obtained at week 0, average percent change in body weight was calculated for each group of Sprague-Dawley (A) and Brown Norway rats (B) every four weeks. $n = 6$, $p < 0.05$. * different from all other groups within the same time point, $ different from both HF diet groups within the same time point, # different from both Reg diet groups within the same time point. (For interpretation of the references to colour in this figure legend, the reader is referred to the web version of this article.)

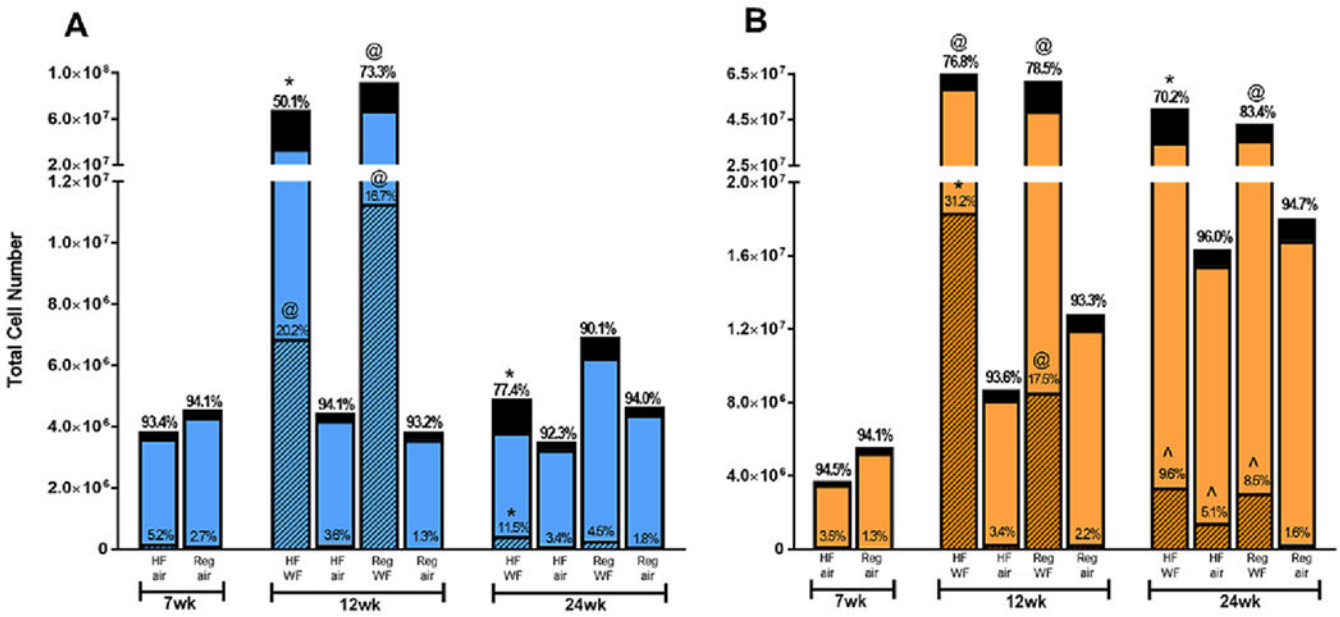

Fig. 3.

Absolute cell number and activation status of alveolar macrophages retrieved by bronchoalveolar lavage (BAL) in Sprague-Dawley (A) and Brown Norway (B) rats. The total number of BAL cells acquired from each group of animals is indicated by the maximum height of the bars on the graph. The orange (SD) and blue (BN) segments of each bar reflect the portion of the total BAL cell pool comprised of alveolar macrophages (also indicated by the values listed above the entire bar) and the black portion reflects the prevalence of all other cellular constituents in the BAL. Within the colored segment of the bars, the hatched portion represents the proportionality of alveolar macrophages expressing an activated phenotype ($MHCII^{hi}$). The prevalence of activated macrophages within the BAL is also denoted by the percentage listed above the hatched portion of the bar for each group and time point, $n = 6$, $p < 0.05$. * different from all other groups within the same time point; @ different from both all-exposed groups within the same time point. (For interpretation of the references to colour in this figure legend, the reader is referred to the web version of this article.)

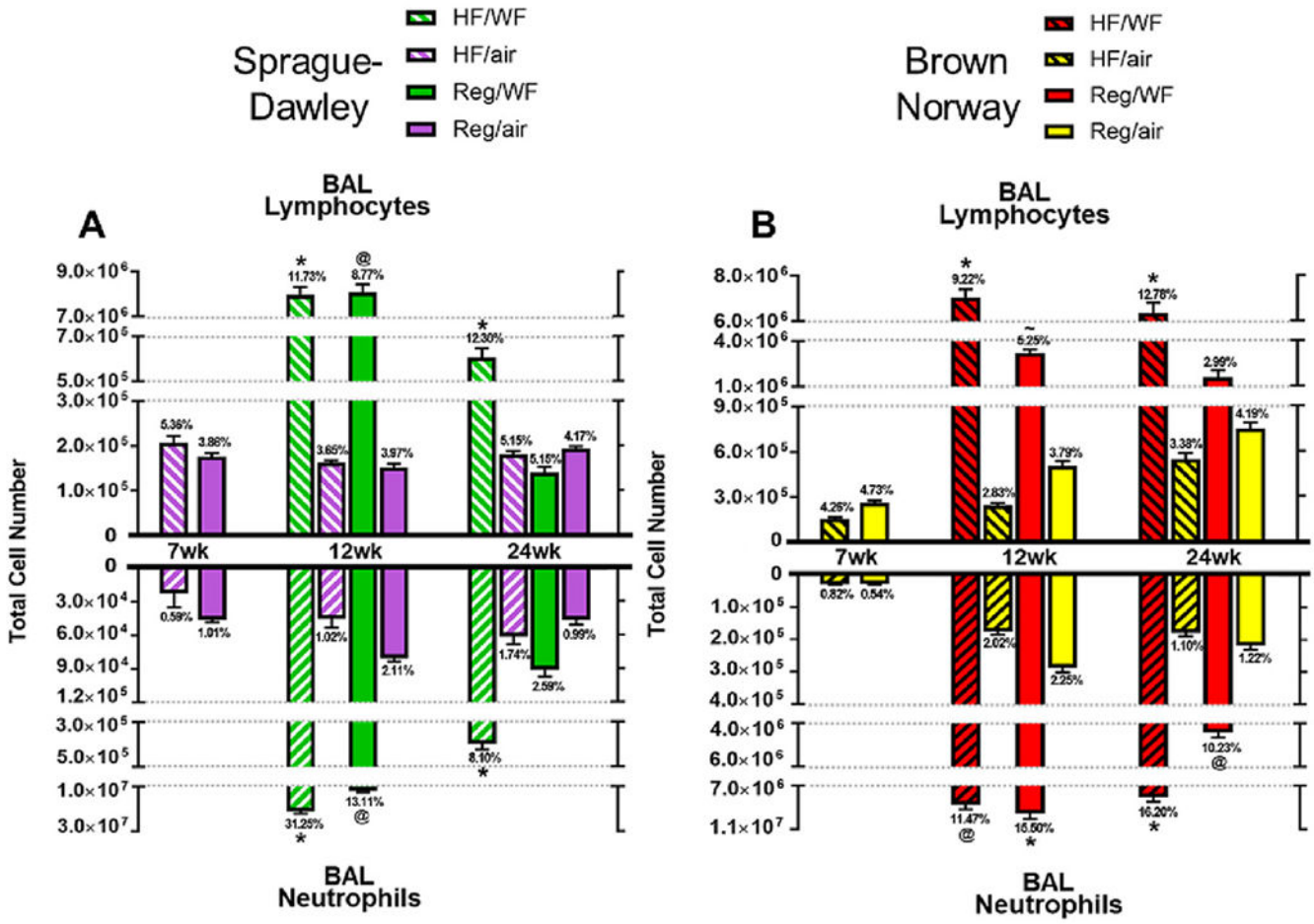

Fig. 4.

Quantification of lymphocytes and neutrophils in the bronchoalveolar lavage (BAL) of Sprague-Dawley (A) and Brown Norway (B) rats. The bars on the graph indicate absolute numbers of lymphocytes (top) and neutrophils (bottom) obtained from BAL at each time point. Each subpopulation of cells is also expressed as a percentage of the total BAL cell count for the corresponding group and time point, as noted above each bar along with indications of statistical significance $n = 6$, $p < 0.05$. * different from all other groups within the same time point; @ different from both air exposed groups within the same time point. (For interpretation of the references to colour in this figure legend, the reader is referred to the web version of this article.)

A

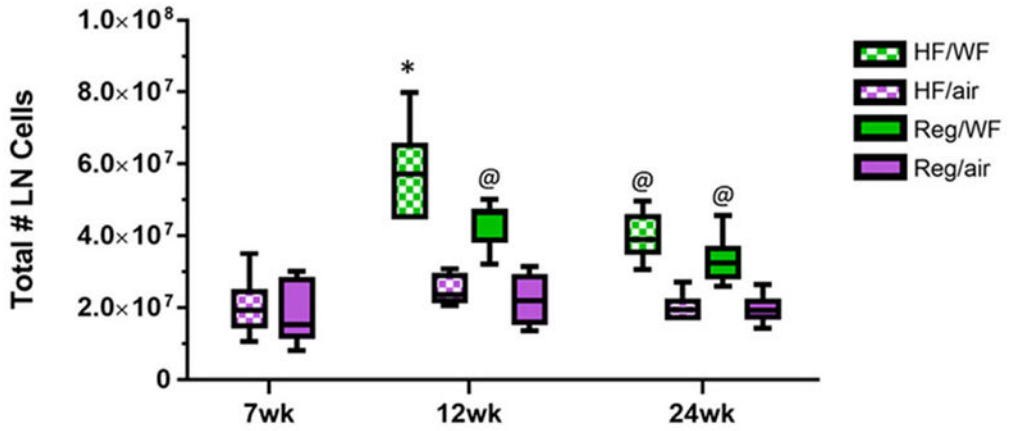

B

Lymph Node Cell Phenotypes by Percent: Sprague-Dawley										
Cell Type	7wk		12wk				24wk			
	HF	Reg	HF/WF	HF/air	Reg/WF	Reg/air	HF/WF	HF/air	Reg/WF	Reg/air
Total # LN Cells	20,248,333	18,159,000	58,181,667*	24,812,167	46,549,000@	22,198,333	39,908,333@	19,995,333	33,216,667@	19,611,667
T-cells	68.41%	74.37%*	63.42%*	71.44%	72.65%	76.38%	64.48%*	72.36%	75.53%	75.03%
CD4+ T-cells	45.97%	48.60%	39.94%*	47.71%	47.35%	49.47%	39.97%*	45.21%	48.75%	48.21%
CD44hi	-	-	34.15%@	3.52%	33.82%@	3.76%	13.06%*	5.31%	7.54%	3.68%
CD8+ T-cells	22.43%	25.77%	23.47%	23.72%	25.30%	26.91%	24.51%	27.15%	26.78%	26.82%
CD44hi	-	-	52.43%*	4.91%	26.44%@	2.53%	27.47%*	5.22%	5.98%	2.91%
CD4:8 Ratio	2.07	1.92	1.77	2.08	1.96	1.85	1.67	1.71	1.83	1.82
B-cells	22.94%*	16.92%	32.92%*	24.15%^	21.41%^	16.03%	31.45%*	16.93%	19.00%	17.18%
CD86hi	-	-	25.10%*	3.26%	10.41%@	1.59%	14.21%*	3.59%	4.57%	2.28%
B:T Ratio	0.34*	0.23	0.53*	0.34^	0.30	0.21	0.49*	0.23	0.25	0.23
NK Cells	0.17%	0.11%	0.41%	0.16%	0.14%	0.10%	0.40%	0.65%	0.22%	0.07%
% Lymphocytes	93.51%	91.40%	94.75%	92.74%	94.20%	92.50%	92.04%	89.94%	94.05%	92.21%
% Non-Lymphoid Cells	6.42%	6.70%	6.15%	5.26%	5.80%	7.11%	7.67%	6.96%	5.26%	7.72%

Fig. 5.

Total cell number (A) and phenotypic differentiation of immune cell subsets (B) within the mediastinal lymph nodes of Sprague Dawley rats at 7, 12, and 24 wks. $n = 6$ $p < 0.05$. * different from all other groups within the same time point; @ different from both air-exposed groups within the same time point; ^ different from Reg/air group within the same time point.

A

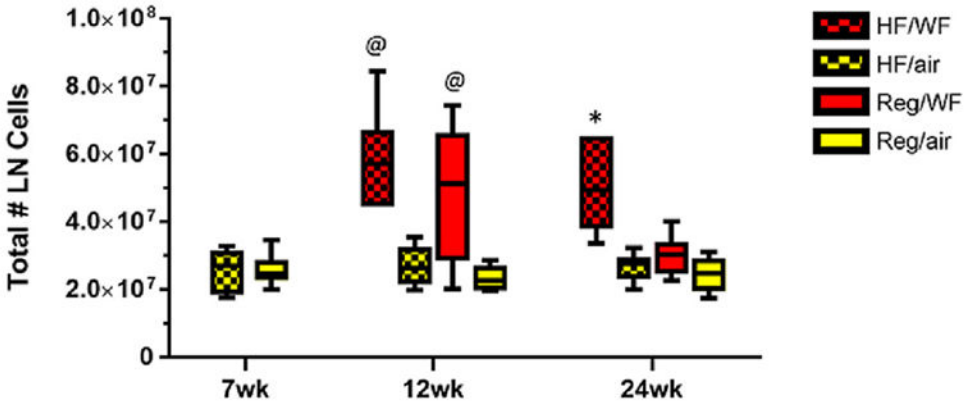

B

Lymph Node Cell Phenotypes by Percent: Brown Norway										
Cell Type	7wk		12wk				24wk			
	HF	Reg	HF/WF	HF/air	Reg/WF	Reg/air	HF/WF	HF/air	Reg/WF	Reg/air
Total # LN Cells	**25,683,333**	**25,641,667**	58,181,667@	26,876,667	53,656,667@	22,280,000	49,283,333*	26,635,000	30,045,000	24,433,333
T-cells	66.14%	68.95%	65.32%	66.63%	67.67%	68.56%	65.58%	67.84%	67.04%	68.50%
CD4+ T-cells	60.93%	62.74%	63.90%	61.80%	61.12%	62.89%	61.53%	62.90%	62.17%	63.15%
CD44hi	0.76%	1.37%	29.95%*	1.92%	23.33%@	1.68%	21.47%*	1.33%	2.63%	1.25%
CD8+ T-cells	5.21%	6.21%	3.42%#	4.83%	6.55%	5.67%	4.05%	4.95%	4.86%	5.35%
CD44hi	0.64%	0.54%	10.67%@	1.04%	9.08%@	1.33%	5.62%*	1.25%	1.71%	1.02%
CD4:8 Ratio	12.24	10.62	18.68*	12.90	9.75	11.39	15.98*	12.74	13.16	12.01
B-cells	22.94%*	16.92%	30.92%*	22.15%^	21.41%^	16.03%	31.45%*	16.93%	19.00%	17.18%
CD86hi	11.81%*	3.77%	51.24%*	9.46%	22.22%@	3.96%	12.39%#	8.43%#	2.39%	3.19%
B:T Ratio	0.43	0.38	0.47	0.40	0.42	0.37	0.43	0.41	0.38	0.40
NK Cells	0.13%	0.18%	0.15%	0.10%	0.20%	0.10%	0.15%	0.13%	0.11%	0.20%
% Lymphocytes	94.95%	95.14%	89.41%	93.04%	91.32%	94.35%	93.12%	95.07%	92.91%	94.73%
% Non-Lymphoid Cells	5.07%	4.16%	7.59%	6.76%	5.63%	5.16%	6.09%	4.53%	7.01%	4.27%

Fig. 6.

Total cell number (A) and phenotypic differentiation of immune cell subsets (B) within the lymph nodes of Brown Norway rats at 7, 12, and 24 wk. $n = 6$, $p < 0.05$. * different from all other groups within the same time point; @ different from both air-exposed groups within the same time point; # different from both Reg diet groups within the same time point; ^ different from Reg/air group within the same time point. (For interpretation of the references to colour in this figure legend, the reader is referred to the web version of this article.)

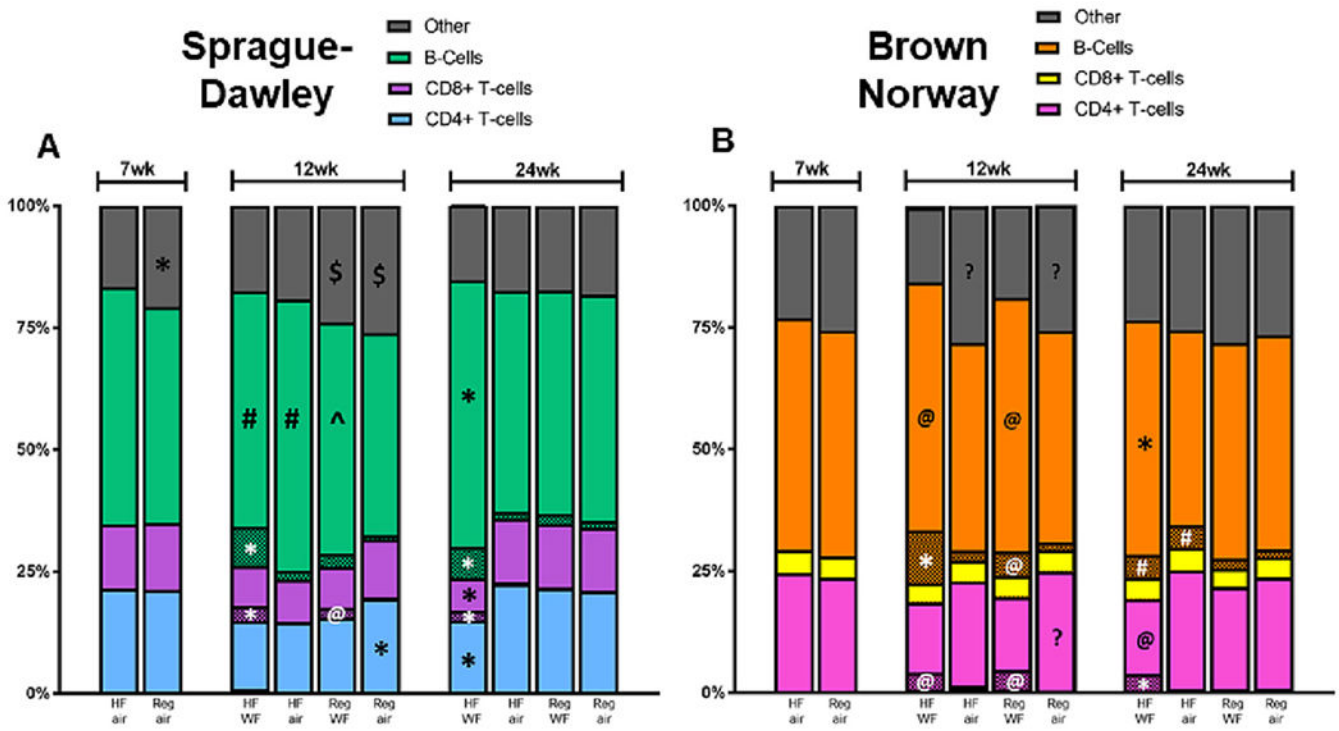

Fig. 7.

Phenotypic profile of splenic lymphocytes in Sprague Dawley (A) and Brown Norway (B) rats. Frequencies of CD4+ T-cells (blue, pink), CD8+ T-cells (purple, yellow), B-cells (green, orange), and other cells (gray, NK cells + non-lymphoid cells) are shown as a percentage of the total splenocyte pool for each group at 7, 12, and 24 wk., wherein statistically significant differences in these subpopulations are denoted by the black symbols within the corresponding-colored bars For each lymphocyte subpopulation, the proportion of cells expressing an activated phenotype is indicated by the shaded portion of the same-colored bar and statistical significance is shown in white text. $n = 6$, $p < 0.05$. * different from all other groups within the same time point, # different from both Reg diet groups within the same time point; $ different from both HF diet groups within the same time point; @ different from both air-exposed groups within the same time point; different from Reg/air group within the same time point. (For interpretation of the references to colour in this figure legend, the reader is referred to the web version of this article.)

A

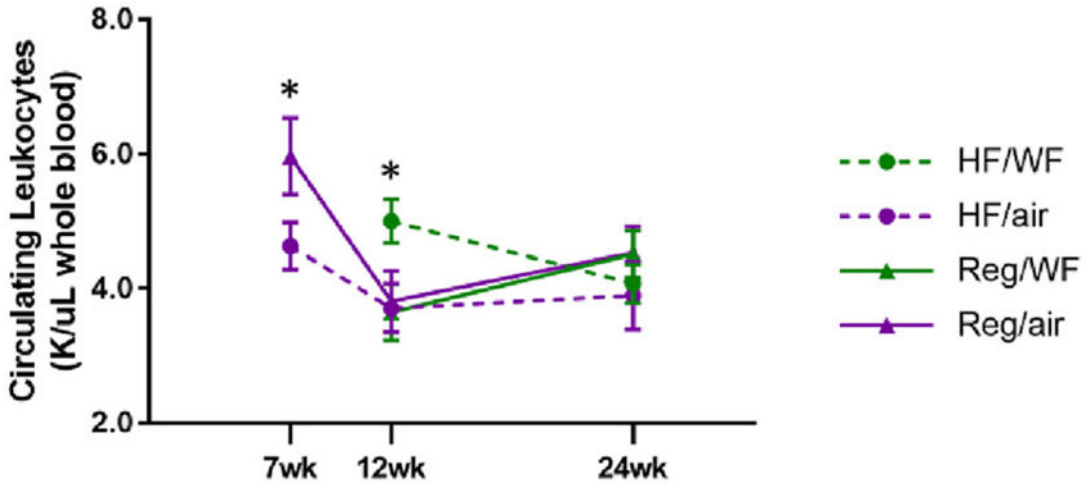

B

Circulating Leukocyte Populations by Absolute Number and Percent: Sprague-Dawley

		# WBC (k/uL)					Total WBC	% WBC				
		Neutr	Lymph	Mono	Eos	Baso	(K/uL)	Neutr	Lymph	Mono	Eos	Baso
7wk	HF	0.97	3.39	0.15	0.11	0.01	**4.63***	21.0%*	73.2%*	3.2%	2.4%	0.2%
	Reg	0.83	4.68	0.25	0.13	0.01	**5.90**	14.1%	79.3%	4.2%	2.2%	0.2%
12wk	HF/WF	0.97	3.80	0.17	0.09	0.00	**5.03***	19.3%#	75.5%	3.4%	1.8%	0.0%
	HF/air	0.70	2.74	0.14	0.11	0.01	**3.70**	18.9%#	74.1%	3.8%	3.0%	0.3%
	Reg/WF	0.38	3.07	0.08	0.10	0.00	**3.63**	10.5%	84.6%$	2.2%	2.8%	0.0%
	Reg/air	0.42	3.20	0.12	0.08	0.02	**3.84**	10.9%	83.3%$	3.1%	2.1%	0.5%
24wk	HF/WF	0.76	2.97	0.23	0.10	0.01	**4.07**	18.7%	73.0%	5.7%	2.5%	0.2%
	HF/air	0.85	2.67	0.27	0.08	0.01	**3.88**	21.9%#	68.8%#	7.0%	2.1%	0.3%
	Reg/WF	0.65	3.58	0.20	0.08	0.01	**4.52**	14.4%	79.2%	4.4%	1.8%	0.2%
	Reg/air	0.75	3.44	0.20	0.11	0.01	**4.51**	16.6%	76.3%	4.4%	2.4%	0.2%

Fig. 8.

Blood leukocyte profile of Sprague-Dawley rats at 7, 12, and 24 wk. The total number of circulating leukocytes (WBC) was determined for each group and is reported in thousands of cells per microliter of whole blood (A). Phenotypic differentiation of neutrophils, lymphocytes, monocytes, eosinophils, and basophils within the pool of circulating leukocytes was also performed (B). Absolute number is shown for each immune cell subset, in addition to population frequency expressed as a percentage of total blood leukocytes. $n = 6$, $p < 0.05$. * different from all other groups within the same time point; # different from both Reg diet groups within the same time point; $ different from both HF diet groups within the same time point.

A

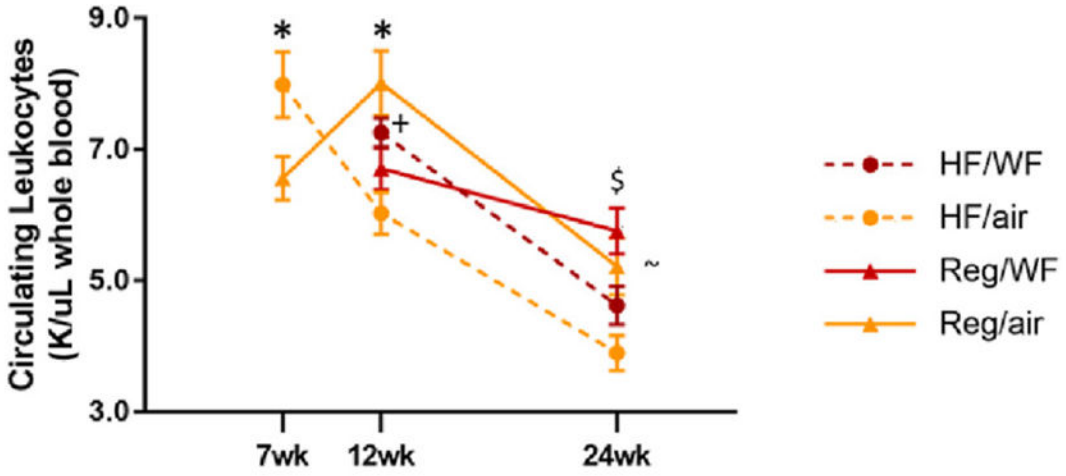

B

Circulating Leukocyte Populations by Absolute Number and Percent: Brown Norway

		# WBC (k/uL)					Total WBC	% WBC				
		Neutr	Lymph	Mono	Eos	Baso	(K/uL)	Neutr	Lymph	Mono	Eos	Baso
7wk	HF	0.68	6.92	0.22	0.14	0.02	**7.98***	8.5%	86.7%	2.8%	1.8%	0.3%
	Reg	0.64	5.61	0.21	0.09	0.01	**6.56**	9.8%	85.5%	3.2%	1.4%	0.2%
12wk	HF/WF	1.02	5.81	0.28	0.15	0.02	**7.28+**	14.0%@	79.8%	3.8%	2.1%	0.3%
	HF/air	0.61	5.00	0.28	0.14	0.01	**6.04**	10.1%	82.8%=	4.6%	2.3%	0.2%
	Reg/WF	1.16	5.25	0.26	0.09	0.00	**6.76**	17.2%@	77.7%	3.8%	1.3%	0.0%
	Reg/air	0.68	6.93	0.30	0.13	0.01	**8.05***	8.4%	86.1%?	3.7%	1.6%	0.1%
24wk	HF/WF	0.99	3.32	0.25	0.06	0.01	**4.63**	21.4%@	71.7%	5.4%	1.3%	0.2%
	HF/air	0.53	3.14	0.15	0.06	0.01	**3.89**	13.6%	80.7%?	3.9%	1.5%	0.3%
	Reg/WF	1.18	4.28	0.23	0.05	0.01	**5.75$**	20.5%@	74.4%	4.0%	0.9%	0.2%
	Reg/air	0.81	4.18	0.19	0.05	0.01	**5.24~**	15.5%	79.8%?	3.6%	1.0%	0.2%

Fig. 9.

Blood leukocyte profile of Brown Norway rats at 7, 12, and 24 wk. The total number of circulating leukocytes (WBC) was determined for each group and is reported in thousands of cells per microliter of whole blood (A). Phenotypic differentiation of neutrophils, lymphocytes monocytes, eosinophils, and basophils within the pool of circulating leukocytes was also performed (B). Absolute number is shown for each immune cell subset, in addition to population frequency expressed as a percentage of total blood leukocytes. $n = 6$, $p < 0.05$. * different from all other groups within the same time point; @ different from both air-exposed groups within the same time point;? different from both WF-exposed groups within the same time point; $ different from both HF diet groups within the same time point; + different from HF/air, Reg/WF groups within the same time point; ~ different from HF/air group within the same time point; = different from Reg/WF group within the same

time point. (For interpretation of the references to colour in this figure legend, the reader is referred to the web version of this article.)

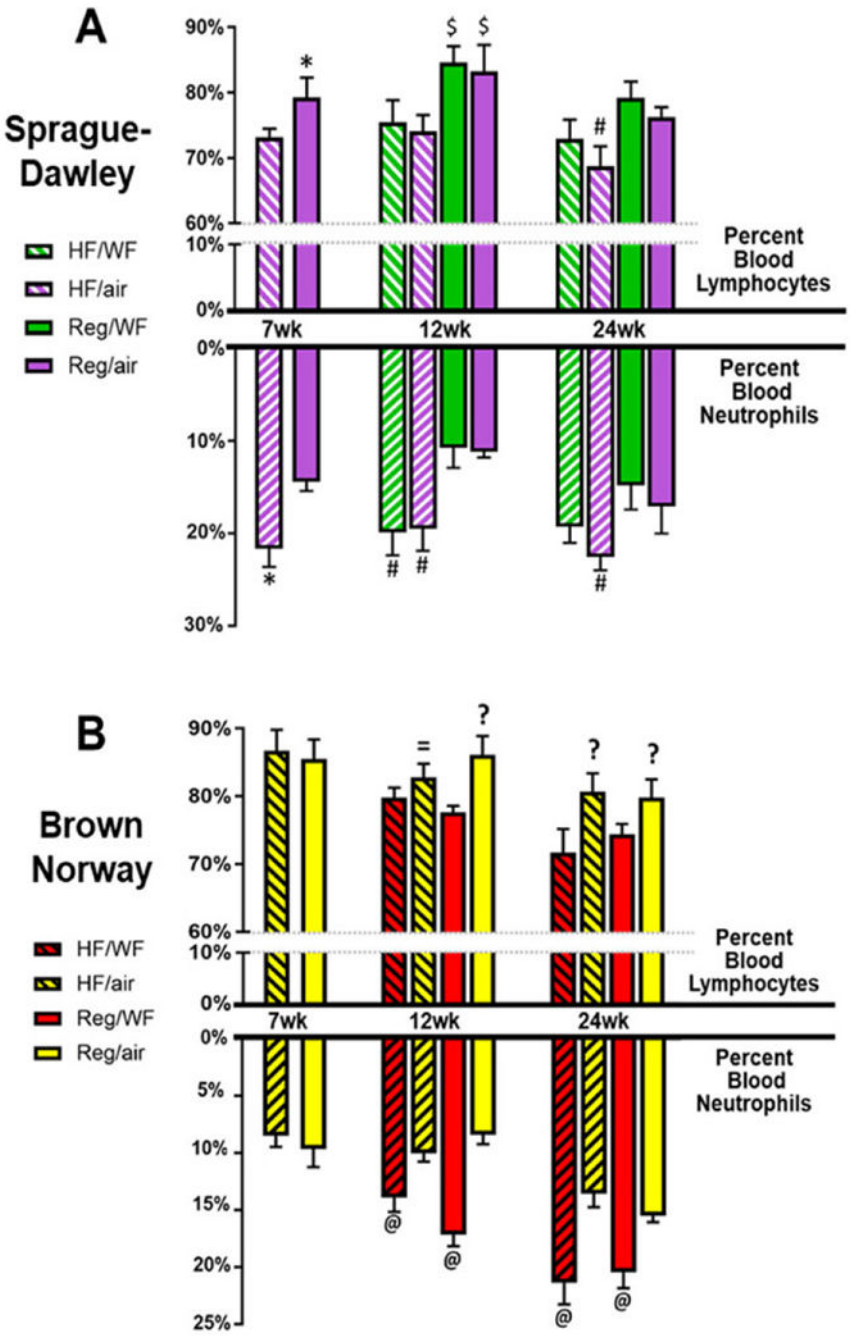

Fig. 10.

Changes in blood lymphocyte and neutrophil populations in Sprague-Dawley (A) and brown Norway (B) rats at 7, 12, and 24 wk The prevalence of each cell subset is expressed as a percentage ot total circulating leukocytes at the corresponding time point. $n = 6$, $p < 0.05$. * different front all other groups within the same time point; # different front both Reg diet groups within the same time point; $ different front both HF diet groups within the same time point. @ different from both air-exposed groups within the same time point;? different front both WF-exposed groups within the same time point; = different front Reg/WF group

within the same time point. (For interpretation of the references to colour in this ligure legend, the reader is referred to the web version of this article.)

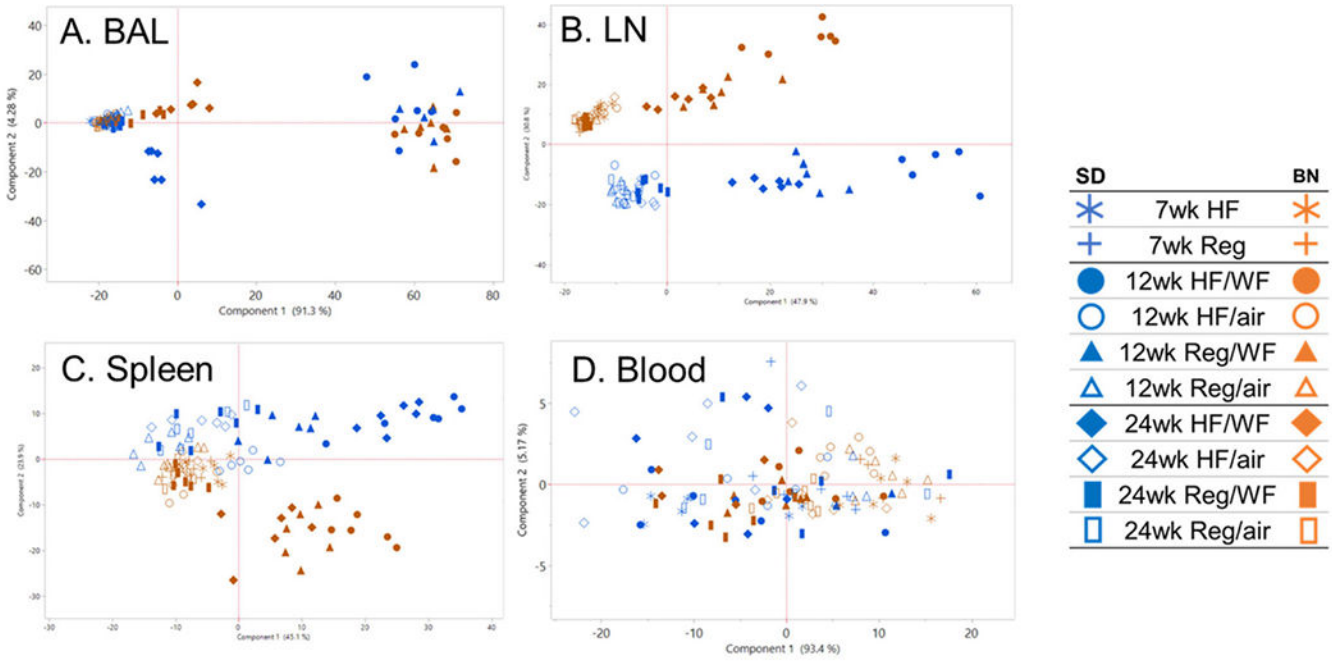

Fig. 11.

Principal Components Analysis plots for tissue specific immune endpoints obtained from bionchoalveolar lavage (BAL, A), lymph nodes (B), spleen (C), and blood (D) in Sprague Dawley (blue icons) and Brown Norway (orange icons) rats at 7, 12, and 24 wk. (For interpretation of the references to colour in this figure legend, the reader is referred to the web version of this article.)

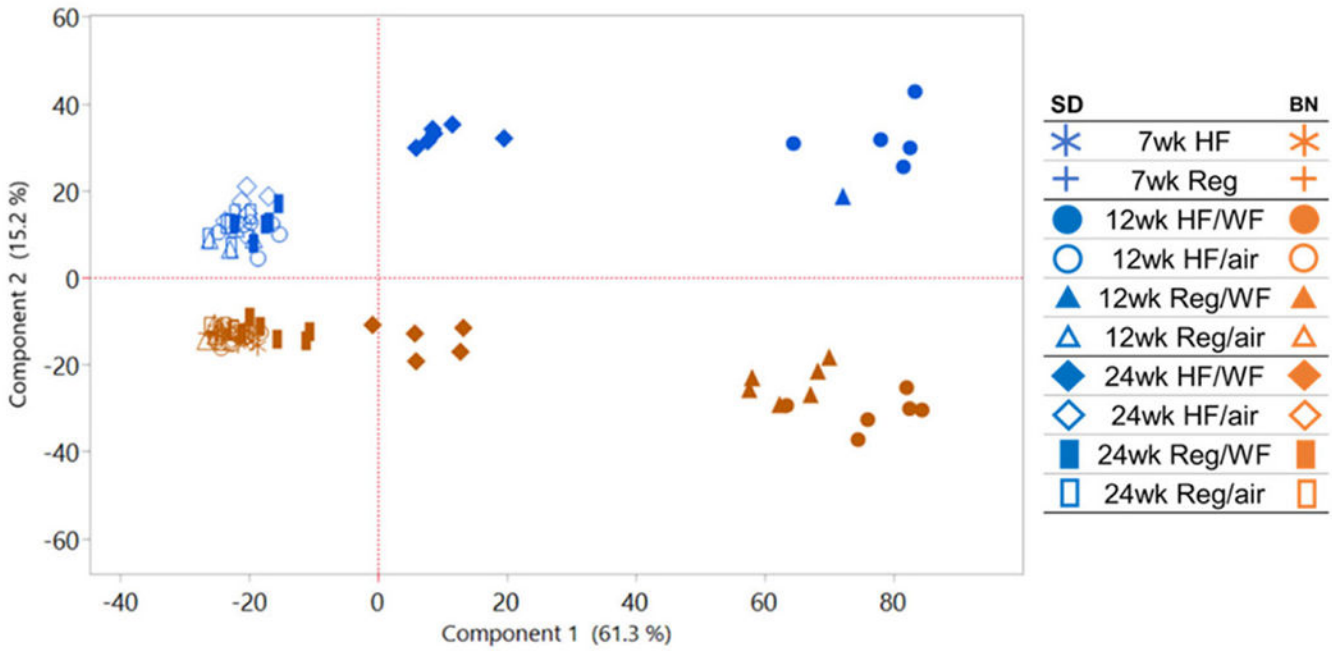

Fig. 12.

Principal Components Analysis summary plot illustrating clustering of all immune-related endpoints collected front Sprague-Dawley (blue icons) and Brown Norway (orange icons) rats at 7, 12, and 24 wk. (For interpretation of the references to colour in this figure legend, the reader is referred to the web version of this article.)